ISSN (Print) 1226-1750
ISSN (Online) 2233-6656
Journal of Magnetics 23(2), 300-311 (2018) https://doi.org/10.4283/JMAG.2018.23.2.300

Analytical Solution of Magnetic Field in High Speed Surface Mounted Permanent Magnet Machine With Parallelly Magnetized Magnet Segments

Shilei Xu[1]* and Xiquan Liu[2]

[1]*Beihang University, Beijing 100083, China*
[2]*Beijing Institute of Control Engineering, Beijing 100080, China*

(Received 28 June 2017, Received in final form 19 March 2018, Accepted 21 March 2018)

Due to some limitations of permanent-magnet (PM) production and magnetizing technology, it is difficult to construct the large magnetic poles of high-power surface-mounted PM machines by using integral magnets. One simple solving scheme is that the large magnetic poles can be formed by several parallelly magnetized magnet segments. For the surface-mounted PM machines with parallelly magnetized magnet segments, this paper gives an accurate analytical solution of the magnetic field. First, in 2-D polar coordinates, the PM machine model is divided into three subdomains, and the magnetic field governing equations are established in each region. By adopting the theory of Fourier's series and the method of separating variables, the solutions of the magnetic field are determined according to associated boundary conditions. Then, the proposed analytical model is compared with finite element method, and the results show that they have a good agreement. Based on the obtained magnetic field solution, the induced electromotive force of a designed PM machine is calculated, and the result is verified by experiment.

Keywords : analytical solution, magnetic field, parallel magnetization, permanent-magnet machine, segmentation

1. Introduction

With the development of rare earth permanent-magnet (PM) materials, the advantages of PM machines become more and more obvious, such as high efficiency, high power density, and low maintenance [1, 2]. For some applications, high-speed PM machines are much preferred, e.g., compressors [3], flywheels [4], machine tools [5], turbo-molecular pumps [6], and so on, because they can further reduce the size and weight of machines, eliminate the link of gear box, and improve the system efficiency and performance [7-9].

The accurate knowledge of magnetic field distribution is fundamental for PM machines design and characteristics investigation. The numerical method, such as finite element method (FEM), has become a very powerful tool in the electromagnetic field analysis, because of its high accuracy and capability of complex structures and nonlinear computations. However, the numerical method usually needs complex process and longer operation time. By contrast, analytical method is more flexible for adjusting design parameters and require shorter computing time. Therefore, the analytical method is useful for preliminary design and optimization of the machines, while the numerical method is good for validation and modification of the designs.

Some comprehensive reviews on analytical computations of magnetic fields in electrical machines can be found in [10, 11]. One of the analytical methods, generally named *Subdomain Model*, can calculate the magnetic field distributions with excellent accuracy. In such model, the whole domain of the electric machine is divided into several regular subdomains, then directly solving the magnetic field governing functions in all subdomains by applying the boundary conditions and obtaining the magnetic field distribution. The method of subdomain model has been used in many electrical machines, in addition to the literatures reviewed in [10] and [11], there are some new contributions in this area. Dubas and Espanet [10] developed an analytical solution taking into account the slotting effect on magnetic field in surface-mounted PM machines, and the developed solution applied to the surface-mounted PM machines with radially or parallelly magnetized magnets. Then, Zhu *et al*. [11] ex-

©The Korean Magnetics Society. All rights reserved.
*Corresponding author: Tel: +8615210923171
e-mail: xushilei@qq.com

© 2018 Journal of Magnetics

tended this subdomain model for computing the magnetic field in surface-mounted PM machines with any pole and slot combinations, including integer slot and fractional slot configurations. This model accurately considered the interaction between stator slots, radial/parallel magnetizations, internal/external rotor topologies, and odd/even periodic boundary conditions. Moreover, the relationship between the exact subdomain model and the subdomain model based on one slot/pole [12, 13] was also discussed. In [10] and [11], the stator slots were modeled as spoke-like shape, and the PM machines were under the no-load condition. Then Lubin *et al*. [14] and Wu *et al*. [15] improved the subdomain mode for the surface-mounted PM machines with semi-closed slots, and the models calculated the armature reaction magnetic field. Afterwards, Lubin *et al*. [16] applied their analytical model on the surface-inset PM machines. Also, Rahideh and Korakianitis [17] presented the analytical calculations of open-circuit and armature reaction field distribution for the slotted machines with surface-inset magnets, and the results of the open-circuit magnetic field in three different magnetization patterns: radial, parallel, and Halbach were given. In addition, Boughrara *et al*. [18] proposed a subdomain model for predicting open-circuit, armature reaction and on-load magnetic fields in integer slot distributed winding parallel double excitation and spoke-type PM machine. Fu and Zhu [19] gave an analysis of the magnetic field distribution induced by rotor eccentricity in slotted surface-mounted PM machines. Shen and Zhu [20] proposed a Halbach PM machines having mixed grade and unequal height of magnets, and analyzed its electromagnetic performance based on subdomain model. Xia *et al*. [21] extended the exact subdomain model to the surface-mounted PM machine with auxiliary slots, and investigated the effects of auxiliary slot parameters on cogging torque. Zhou *et al*. [22] presented an analytical calculation of the magnetic field in surface-mounted PM accounting for eccentric magnets shape, in which the magnets were based on the model of equivalent surface currents

For high-power PM machines, the magnetic poles will be large. It is hard to form such magnetic pole by using single integral magnet, so each magnetic pole can be composed by several pieces of small magnets. This will increase the difficulty of magnets assembly. However, the segmentation of magnets could reduce the eddy current losses in the magnets [23-25], which is beneficial to the high-speed PM machines associated with high loss density and poor cooling conditions. Besides, in practice, radial magnetization of magnets requires more complex process and needs customized magnetizing fixtures for different

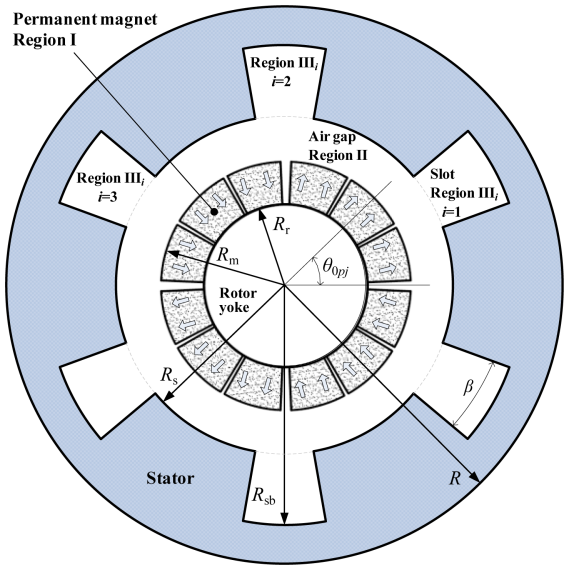

Fig. 1. (Color online) General configuration of the surface-mounted PM machine with parallelly magnetized magnet segments.

sizes of magnets, so the radial magnetization will greatly increase the cost of PMs. Moreover, due to some limitation of magnet production and magnetizing technology, actual performance of magnets by radially magnetized is worse than those by parallelly magnetized. Based on the above reasons, the large poles of high-power PM machines can be formed by several parallelly magnetized segmented magnets, such as shown in the schematic Fig. 1.

As discussed previously, the analytical computations of the magnetic field have been applied in many kinds of electrical machines. However, there is no one appropriate analytical model for this practical PM machine with parallelly magnetized segmented magnets. In this paper, an accurate analytical solution is presented for calculating the magnetic field in surface-mounted PM machines with parallelly magnetized magnet segments configuration, and the performances of the deduced analytical solution are investigated by comparing with FEM. Then, the induced electromotive force (EMF) is calculated based on the obtained magnetic field solution, and the results are verified by measurement. Besides, the other improvements and novelties offered in this paper are as follows. In order to reflect the real conditions, the gaps between the magnet segments caused by septum, glue, or air appeared in actual assembly of magnets are considered in the analytical model, so the calculated results will be more precise. The Fourier's series expansions of all magnetic functions are over entire circumference instead of one pole-pitch, so it makes the solving process more direct and clear, and the present model can be easily extended to other surface-

mounted PM machines.

2. Analytical Solution of the Magnetic Field

The general configuration of the PM machine discussed in this work is shown in Fig. 1. All magnets are magnetized in parallel direction, and each magnetic pole can be composed of several magnet segments depending on specific design and realistic PM production technology. In Fig. 1, the gaps between the magnet segments take into account the existence of septum, glue, or air in actual assembly of magnets. The main geometrical parameters of the PM machine are as follows: R_r is the outer radius of rotor yoke, R_m is the outer radius of magnets, R_s is the inner radius of stator, R_{sb} is the radius of slot bottom, R is the outer radius of stator, and β is the slot opening angle.

To facilitate the analytical modelling, the following assumptions are made: 1) The PMs are uniformly magnetized and have linear demagnetization characteristic. 2) End effects of the magnets and iron cores are neglected. 3) Permeability of stator and rotor iron is infinite. 4) Stator slots are ideal spoke-like shape as shown in Fig. 1. 5) Eddy currents are neglected in all conductive bodies.

As can be seen in Fig. 1, the model of the PM machine can be divided into three types of regions, viz. PM (Region I), air gap (Region II), and stator slots (Region III$_i$, i = 1, 2, …, Q). Owing to the cylindrical machine geometry and the neglect of end effects, the calculation will be solved in 2-D polar coordinates.

2.1. Modeling of PMs

For the PMs having linear demagnetization characteristic, the amplitude of the magnetization vector $\boldsymbol{M}$ is given by

$$M = \frac{B_{rm}}{\mu_0} \tag{1}$$

where B_{rm} is the remanence of PMs, and μ_0 is the permeability of free space. In 2-D polar coordinates, the magnetization vector $\boldsymbol{M}$ can be expressed as

$$\boldsymbol{M} = M_r \boldsymbol{r} + M_\theta \boldsymbol{\theta} \tag{2}$$

where M_r and M_θ are the radial and tangential components of the vector $\boldsymbol{M}$. As an example, Fig. 2 shows the schematic waveforms for M_r and M_θ of the PM configuration presented in Fig. 1. To set up the mathematic expressions, components M_r and M_θ can be expanded as Fourier's series over the entire circumference, i.e.,

$$\begin{aligned} M_r &= \sum_{n=1}^{\infty} M_{rn} \sin\left[\frac{n}{2}(\theta - \omega t - \theta_0)\right] \\ &= \sum_{n=1}^{\infty} M_{rns} \sin\left(\frac{n}{2}\theta\right) + \sum_{n=1}^{\infty} M_{rnc} \cos\left(\frac{n}{2}\theta\right) \end{aligned} \tag{3a}$$

$$\begin{aligned} M_\theta &= \sum_{n=1}^{\infty} M_{\theta n} \cos\left[\frac{n}{2}(\theta - \omega t - \theta_0)\right] \\ &= \sum_{n=1}^{\infty} M_{\theta ns} \sin\left(\frac{n}{2}\theta\right) + \sum_{n=1}^{\infty} M_{\theta nc} \cos\left(\frac{n}{2}\theta\right) \end{aligned} \tag{3b}$$

where

$$M_{rns} = M_{rn} \cos\left[\frac{n}{2}(\omega t + \theta_0)\right] \tag{4a}$$

$$M_{rnc} = -M_{rn} \sin\left[\frac{n}{2}(\omega t + \theta_0)\right] \tag{4b}$$

$$M_{\theta ns} = M_{\theta n} \sin\left[\frac{n}{2}(\omega t + \theta_0)\right] \tag{4c}$$

$$M_{\theta nc} = M_{\theta n} \cos\left[\frac{n}{2}(\omega t + \theta_0)\right] \tag{4d}$$

where θ is the mechanical angular position; θ_0 is the initial angular position of the rotor; ω and t are the angular velocity and rotation time of the rotor, respectively.

For the discussed PM configuration with parallelly magnetized magnet segments, the Fourier coefficients can be expressed as

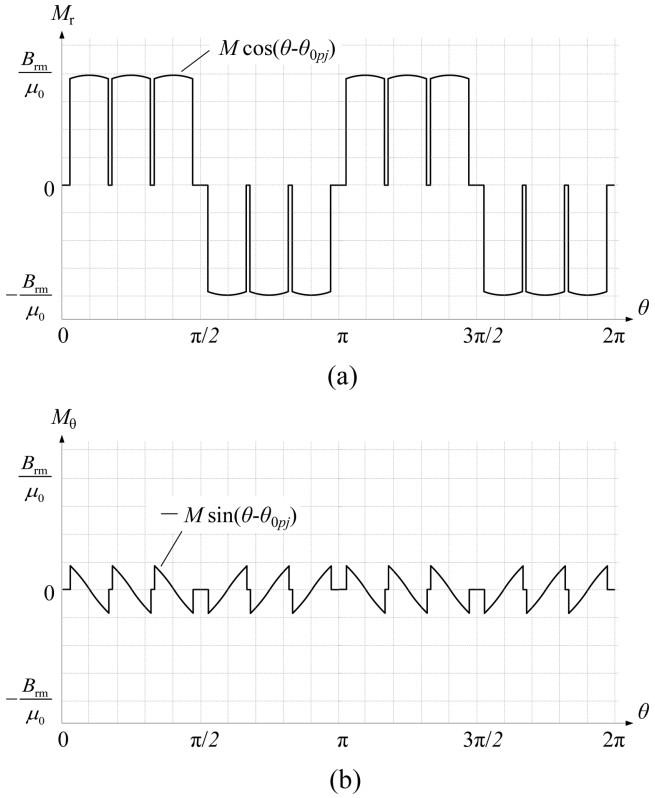

Fig. 2. Schematic waveforms for the radial and tangential components of the magnetization vector (a) Radial component M_r (b) Tangential component M_θ.

$$M_{rn} = \frac{1}{\pi}\sum_{p=1}^{2P}\left[(-1)^{p+1}\sum_{j=1}^{J}\int_{\theta_{0pj}-\frac{\theta_m}{2}}^{\theta_{0pj}+\frac{\theta_m}{2}} M\cos(\theta-\theta_{0pj})\sin\left(\frac{n}{2}\theta\right)\mathrm{d}\theta\right] \quad (5a)$$

$$M_{\theta n} = \frac{1}{\pi}\sum_{p=1}^{2P}\left[(-1)^{p}\sum_{j=1}^{J}\int_{\theta_{0pj}-\frac{\theta_m}{2}}^{\theta_{0pj}+\frac{\theta_m}{2}} M\sin(\theta-\theta_{0pj})\cos\left(\frac{n}{2}\theta\right)\mathrm{d}\theta\right] \quad (5b)$$

where

$$\theta_{0pj} = \theta_{0p} + \left(j-\frac{1}{2}\right)\frac{\pi\lambda_p}{PJ} \quad (6a)$$

$$\theta_{0p} = \frac{1}{2}\frac{\pi}{P}(1-\lambda_p) + (p-1)\frac{\pi}{P} \quad (6b)$$

$$\theta_m = \frac{\pi\lambda_p\lambda_m}{PJ} \quad (7)$$

where θ_{0pj} is the mechanical angular position of magnetization direction of the jth magnet in the pth pole, θ_{0p} is the starting angular position of the pth magnetic pole, θ_m is the mechanical angle of the segmented magnet arc, P is the number of pole pairs, J is the number of segmented magnets in the pole, λ_p is the ratio of pole-arc to pole-pitch, and λ_m is the ratio of magnet-arc to magnet-pitch.

Note that the magnetization only exists in the magnets. For the space without magnets in the region I, it is assumed to be occupied by unmagnetized magnets, i.e., $\boldsymbol{M} = 0$ ($M_r = M_\theta = 0$).

By solving (5), the explicit expressions of the Fourier coefficients are obtained:

$$M_{rn} = \begin{cases} \dfrac{1}{\pi}\displaystyle\sum_{p=1}^{2P}\left\{(-1)^{p+1}\sum_{j=1}^{J}-4M\frac{\left[2\sin\left(\frac{\theta_m}{2}\right)\cos\left(\frac{n\theta_m}{4}\right)-n\cos\left(\frac{\theta_m}{2}\right)\sin\left(\frac{n\theta_m}{4}\right)\right]\sin\left(\frac{n\theta_{0pj}}{2}\right)}{n^2-4}\right\}, \\ \qquad n=1,3,4,\ldots \\ \dfrac{1}{\pi}\displaystyle\sum_{p=1}^{2P}\left\{(-1)^{p+1}\sum_{j=1}^{J}M\left[\frac{\theta_m+\sin(\theta_m)}{2}\right]\sin(\theta_{0pj})\right\}, n=2 \end{cases} \quad (8a)$$

$$M_{\theta n} = \begin{cases} \dfrac{1}{\pi}\displaystyle\sum_{p=1}^{2P}\left\{(-1)^{p}\sum_{j=1}^{J}-4M\frac{\left[2\cos\left(\frac{\theta_m}{2}\right)\sin\left(\frac{n\theta_m}{4}\right)-n\sin\left(\frac{\theta_m}{2}\right)\cos\left(\frac{n\theta_m}{4}\right)\right]\sin\left(\frac{n\theta_{0pj}}{2}\right)}{n^2-4}\right\}, \\ \qquad n=1,3,4,\ldots \\ \dfrac{1}{\pi}\displaystyle\sum_{p=1}^{2P}\left\{(-1)^{p}\sum_{j=1}^{J}-M\left[\frac{\theta_m-\sin(\theta_m)}{2}\right]\sin(\theta_{0pj})\right\}, n=2 \end{cases} \quad (8b)$$

2.2. Magnetic field governing equations

In the discussed model of PM machine, magnetic flux density vector $\boldsymbol{B}$ and magnetic field intensity vector $\boldsymbol{H}$ are coupled by the following relations:

$$\boldsymbol{B}_{\mathrm{I}} = \mu_0\mu_{\mathrm{rm}}\boldsymbol{H}_{\mathrm{I}} + \mu_0\boldsymbol{M} \quad \text{in the PMs} \quad (9a)$$

$$\boldsymbol{B}_{\mathrm{II}} = \mu_0\boldsymbol{H}_{\mathrm{II}} \quad \text{in the air gap} \quad (9b)$$

$$\boldsymbol{B}_{\mathrm{III}i} = \mu_0\boldsymbol{H}_{\mathrm{III}i} \quad \text{in the } i\text{th slot} \quad (9c)$$

where μ_{rm} is the relative recoil permeability of PMs; the subscripts I, II and IIIi denote the PM, air gap, and the ith slot region respectively.

Magnetic flux density vector $\boldsymbol{B}$ can be described by magnetic vector potential $\boldsymbol{A}$:

$$\boldsymbol{B} = \nabla\times\boldsymbol{A} \quad (10)$$

The point form of Ampère's circuital law is given by

$$\nabla\times\boldsymbol{H} = \boldsymbol{J} \quad (11)$$

Performing the curl operation on (9), and taking (10) and (11) into them, then the following equations can be deduced:

$$\nabla\times(\nabla\times\boldsymbol{A}_{\mathrm{I}}) = \mu_0\mu_{\mathrm{rm}}\boldsymbol{J}_{\mathrm{I}} + \mu_0\nabla\times\boldsymbol{M} \quad (12a)$$

$$\nabla\times(\nabla\times\boldsymbol{A}_{\mathrm{II}}) = \mu_0\boldsymbol{J}_{\mathrm{II}} \quad (12b)$$

$$\nabla\times(\nabla\times\boldsymbol{A}_{\mathrm{III}i}) = \mu_0\boldsymbol{J}_{\mathrm{III}i} \quad (12c)$$

There are no conduction currents in PM, air gap, and slots region for no-load operation, so $\boldsymbol{J}_{\mathrm{I}} = \boldsymbol{J}_{\mathrm{II}} = \boldsymbol{J}_{\mathrm{III}i} = 0$. Under the Coulomb gauge

$$\nabla\cdot\boldsymbol{A} = 0 \quad (13)$$

and the relation

$$\nabla\times(\nabla\times\boldsymbol{A}) = \nabla(\nabla\cdot\boldsymbol{A}) - \nabla^2\boldsymbol{A} \quad (14)$$

then (12) can be written as

$$\nabla^2\boldsymbol{A}_{\mathrm{I}} = -\mu_0\nabla\times\boldsymbol{M} \quad (15a)$$

$$\nabla^2\boldsymbol{A}_{\mathrm{II}} = 0 \quad (15b)$$

$$\nabla^2\boldsymbol{A}_{\mathrm{III}i} = 0 \quad (15c)$$

For the discussed 2-D PM machine model, magnetic vector potential $\boldsymbol{A}$ points to Z-direction; in other words, the magnetic vector potential $\boldsymbol{A}$ has only one component A_z along Z-direction, which depends on variables r and θ. Therefore, in the 2-D polar coordinates, magnetic field governing equations (15) can be expressed as

$$\frac{\partial A_{\mathrm{I}}}{\partial r^2} + \frac{1}{r}\frac{\partial A_{\mathrm{I}}}{\partial r} + \frac{1}{r^2}\frac{\partial^2 A_{\mathrm{I}}}{\partial\theta^2} = -\frac{\mu_0}{r}\left(M_\theta - \frac{\partial M_r}{\partial\theta}\right) \quad (16a)$$

$$\frac{\partial A_{\mathrm{II}}}{\partial r^2} + \frac{1}{r}\frac{\partial A_{\mathrm{II}}}{\partial r} + \frac{1}{r^2}\frac{\partial^2 A_{\mathrm{II}}}{\partial\theta^2} = 0 \quad (16b)$$

$$\frac{\partial A_{\mathrm{III}i}}{\partial r^2} + \frac{1}{r}\frac{\partial A_{\mathrm{III}i}}{\partial r} + \frac{1}{r^2}\frac{\partial^2 A_{\mathrm{III}i}}{\partial\theta^2} = 0 \quad (16c)$$

For the sake of clarity and simplicity, the subscript Z in A is omitted here.

It can be seen from (16) that the distribution of magnetic vector potential in the PM region is governed by Poisson's equation, in the air gap region and slots region are governed by Laplace's equation. Once the distributions of magnetic vector potential are obtained, the radial and tangential components of magnetic flux density $\boldsymbol{B}$ can be calculated by

$$B_{\mathrm{r}} = \frac{1}{r}\frac{\partial A}{\partial \theta} \tag{17a}$$

$$B_{\theta} = -\frac{\partial A}{\partial r} \tag{17b}$$

Meanwhile, the magnetic field intensity $\boldsymbol{H}$ can be obtained. Hence, the next task is to solve these magnetic field governing equations.

2.3. General solution of magnetic field equations

1) In PM region

From equations of M_{r} (3a) and M_{θ} (3b), the right side of (16a) can be further written as

$$\begin{aligned} -\frac{\mu_0}{r}\left(M_{\theta} - \frac{\partial M_{\mathrm{r}}}{\partial \theta}\right) &= \sum_{n=1}^{\infty} -\frac{\mu_0}{r}\left(M_{\theta ns} + \frac{n}{2}M_{rnc}\right)\sin\left(\frac{n}{2}\theta\right) \\ &+ \sum_{n=1}^{\infty} -\frac{\mu_0}{r}\left(M_{\theta nc} - \frac{n}{2}M_{rns}\right)\cos\left(\frac{n}{2}\theta\right) \end{aligned} \tag{18}$$

According to the expression shown in the right side of (18), and based on the method of the separation of variables, the solution of Poisson's equation (16a) is assumed as

$$A_{\mathrm{I}}(r,\theta) = \sum_{n=1}^{\infty} f_n(r)\sin\left(\frac{n}{2}\right) + \sum_{n=1}^{\infty} g_n(r)\cos\left(\frac{n}{2}\right) \tag{19}$$

where $f_{\mathrm{n}}(r)$ and $g_{\mathrm{n}}(r)$ are only related to the variable r. Then put (19) back into (16a), the following differential equations can be obtained:

$$f_n''(r) + \frac{1}{r}f_n'(r) - \frac{1}{r^2}\left(\frac{n}{2}\right)^2 f_n(r) = -\frac{\mu_0}{r}\left(M_{\theta ns} + \frac{n}{2}M_{rnc}\right) \tag{20a}$$

$$g_n''(r) + \frac{1}{r}g_n'(r) - \frac{1}{r^2}\left(\frac{n}{2}\right)^2 g_n(r) = -\frac{\mu_0}{r}\left(M_{\theta nc} - \frac{n}{2}M_{rns}\right) \tag{20b}$$

By solving these differential equations can gain

$$f_n(r) = \begin{cases} E_{1n}r^{\frac{n}{2}} + F_{1n}r^{-\frac{n}{2}} + \dfrac{2\mu_0(2M_{\theta ns} + nM_{rnc})}{n^2 - 2^2}r, n = 1,3,4,... \\ E_{1n}r + F_{1n}r^{-1} - \dfrac{\mu_0(M_{\theta ns} + M_{rnc})}{2}r\ln(r), n = 2 \end{cases} \tag{21a}$$

$$g_n(r) = \begin{cases} C_{1n}r^{\frac{n}{2}} + D_{1n}r^{-\frac{n}{2}} + \dfrac{2\mu_0(2M_{\theta nc} - nM_{rns})}{n^2 - 2^2}r, n = 1,3,4,... \\ C_{1n}r + D_{1n}r^{-1} - \dfrac{\mu_0(M_{\theta nc} - M_{rns})}{2}r\ln(r), n = 2 \end{cases} \tag{21b}$$

Thus, the general solution of magnetic field governing equation in PM region is acquired.

2) In air gap region

Similarly, following the above solving process, the general solution of magnetic field governing equation in air gap region can be deduced:

$$\begin{aligned} A_{\mathrm{II}}(r,\theta) &= \sum_{n=1}^{\infty}\left(E_{\mathrm{II}n}r^{\frac{n}{2}} + F_{\mathrm{II}n}r^{-\frac{n}{2}}\right)\sin\left(\frac{n}{2}\theta\right) \\ &+ \sum_{n=1}^{\infty}\left(C_{\mathrm{II}n}r^{\frac{n}{2}} + D_{\mathrm{II}n}r^{-\frac{n}{2}}\right)\cos\left(\frac{n}{2}\theta\right) \end{aligned} \tag{22}$$

3) In slots region

Under the no-load condition of PM machine, the general solution of magnetic field governing equation in stator slots region is given by [26]

$$A_{\mathrm{III}i}(r,\theta) = \sum_{k=1}^{\infty}\left(C_{\mathrm{III}ik}r^{\frac{k\pi}{\beta}} + D_{\mathrm{III}ik}r^{-\frac{k\pi}{\beta}}\right)\cos\left[\frac{k\pi}{\beta}(\theta - \theta_i)\right],$$
$$i = 1, 2, \ldots, Q \;\&\; \theta_i \le \theta \le \theta_i + \beta \tag{23}$$

where θ_i is the starting angular position of the ith slot.

Since the stator is assumed with infinite permeability, the magnetic field lines are perpendicular to the surface of each slot bottom; there is

$$B_{\theta\,\mathrm{III}i}(R_{\mathrm{sb}}) = -\left.\frac{\partial A_{\mathrm{III}i}}{\partial r}\right|_{r=R_{\mathrm{sb}}} = 0 \tag{24}$$

Imposing this condition on (23) yields

$$C_{\mathrm{III}ik} = D_{\mathrm{III}ik}R_{\mathrm{sb}}^{-2Y_k} \tag{25}$$

where

$$Y_k = \frac{k\pi}{\beta} \tag{26}$$

According to (25), (23) can be simplified as

$$\begin{aligned} A_{\mathrm{III}i}(r,\theta) &= \sum_{k=1}^{\infty} D_{\mathrm{III}ik}R_{\mathrm{sb}}^{-Y_k}\left[\left(\frac{r}{R_{\mathrm{sb}}}\right)^{Y_k} + \left(\frac{r}{R_{\mathrm{sb}}}\right)^{-Y_k}\right]\cos[Y_k(\theta - \theta_i)] \\ &= \sum_{k=1}^{\infty} G_{\mathrm{III}ik}\left[\left(\frac{r}{R_{\mathrm{sb}}}\right)^{Y_k} + \left(\frac{r}{R_{\mathrm{sb}}}\right)^{-Y_k}\right]\cos[Y_k(\theta - \theta_i)] \end{aligned}, \tag{27}$$
$$i = 1, 2, \ldots, Q \;\&\; \theta_i \le \theta \le \theta_i + \beta$$

In the above expressions of A_{I} (19), A_{II} (22), and $A_{\mathrm{III}i}$ (27), $C_{\mathrm{I}n}$, $D_{\mathrm{I}n}$, $E_{\mathrm{I}n}$, $F_{\mathrm{I}n}$, $C_{\mathrm{II}n}$, $D_{\mathrm{II}n}$, $E_{\mathrm{II}n}$, $F_{\mathrm{II}n}$ and $G_{\mathrm{III}ik}$ are arbitrary constants to be determined by applying appropriate boundary conditions.

2.4. Magnetic field boundary conditions

At the interface between two different media, the normal components of flux density on two sides are continuous, and the tangential component of magnetic field intensity on one side is equal to that on the other side. For the discussed PM machine model, the boundary conditions are as follows.

1) At the interface between rotor yoke and PM region

Since the rotor yoke is assumed with infinite permeability, the tangential component of magnetic field intensity at this interface is zero, i.e.,

$$H_{\theta \mathrm{I}} = 0,\ r = R_{\mathrm{r}} \tag{28}$$

where

$$H_{\theta \mathrm{I}} = \frac{1}{\mu_0 \mu_{\mathrm{rm}}}\left(-\frac{\partial A_{\mathrm{I}}}{\partial r} - \mu_0 M_{\theta}\right) \tag{29}$$

This means

$$\frac{\partial A_I}{\partial r} + \mu_0 M_{\theta} = 0\,,\ r = R_{\mathrm{r}} \tag{30}$$

Substituting the expressions of A_{I} (19) and M_{θ} (3b) into the condition (30), the following relations are deduced:

$$f_n'(R_r) + \mu_0 M_{\theta ns} = 0 \tag{31a}$$

$$g_n'(R_r) + \mu_0 M_{\theta nc} = 0 \tag{31b}$$

2) At the interface between PM and air gap region

a) The tangential components of magnetic field intensity on two sides of this interface are equal, i.e.,

$$H_{\theta \mathrm{I}} = H_{\theta \mathrm{II}},\ r = R_{\mathrm{m}} \tag{32}$$

It means

$$\frac{1}{\mu_{\mathrm{rm}}}\left(\frac{\partial A_{\mathrm{I}}}{\partial r} + \mu_0 M_{\theta}\right) = \frac{\partial A_{\mathrm{II}}}{\partial r}\,,\ r = R_{\mathrm{m}} \tag{33}$$

Substituting the expressions of A_{I} (19), A_{II} (22) and M_{θ} (3b) into the condition (33), the following relations are obtained:

$$\frac{1}{\mu_{\mathrm{rm}}}[f_n'(R_{\mathrm{m}}) + \mu_0 M_{\theta ns}] = \frac{n}{2}\left(E_{\mathrm{II}n} R_{\mathrm{m}}^{\frac{n}{2}-1} - F_{\mathrm{II}n} R_{\mathrm{m}}^{-\frac{n}{2}-1}\right) \tag{34a}$$

$$\frac{1}{\mu_{\mathrm{rm}}}[g_n'(R_{\mathrm{m}}) + \mu_0 M_{\theta nc}] = \frac{n}{2}\left(C_{\mathrm{II}n} R_{\mathrm{m}}^{\frac{n}{2}-1} - D_{\mathrm{II}n} R_{\mathrm{m}}^{-\frac{n}{2}-1}\right) \tag{34b}$$

b) The radial components of flux density are continuous across this interface, i.e.,

$$B_{\mathrm{rI}} = B_{\mathrm{rII}},\ r = R_{\mathrm{m}} \tag{35}$$

Hence, there is

$$\frac{\partial A_{\mathrm{I}}}{\partial \theta} = \frac{\partial A_{\mathrm{II}}}{\partial \theta}\,,\ r = R_{\mathrm{m}} \tag{36}$$

Substituting the expressions of A_{I} (19) and A_{II} (22) into the condition (36), the following relations are deduced:

$$f_n(R_{\mathrm{m}}) = E_{\mathrm{II}n} R_{\mathrm{m}}^{\frac{n}{2}} + F_{\mathrm{II}n} R_{\mathrm{m}}^{-\frac{n}{2}} \tag{37a}$$

$$g_n(R_{\mathrm{m}}) = C_{\mathrm{II}n} R_{\mathrm{m}}^{\frac{n}{2}} + D_{\mathrm{II}n} R_{\mathrm{m}}^{-\frac{n}{2}} \tag{37b}$$

3) At the interface between air gap and stator

a) At the entire circumference of this interface, the tangential components of magnetic field intensity on two sides are equal, i.e.,

$$H_{\theta \mathrm{II}} = H_{\theta \mathrm{III}},\ r = R_{\mathrm{s}} \tag{38}$$

On the air gap side, the tangential component of magnetic field intensity is

$$\begin{aligned} H_{\mathrm{II}}(R_{\mathrm{s}}) &= -\frac{1}{\mu_0}\frac{\partial A_{\mathrm{II}}}{\partial r}\bigg|_{r=R_{\mathrm{s}}} \\ &= -\frac{1}{\mu_0}\left[\sum_{n=1}^{\infty}\frac{n}{2}\left(E_{\mathrm{II}n} R_{\mathrm{s}}^{\frac{n}{2}-1} - F_{\mathrm{II}n} R_{\mathrm{s}}^{-\frac{n}{2}-1}\right)\sin\left(\frac{n}{2}\theta\right)\right. \\ &\quad \left. + \sum_{n=1}^{\infty}\frac{n}{2}\left(C_{\mathrm{II}n} R_{\mathrm{s}}^{\frac{n}{2}-1} - D_{\mathrm{II}n} R_{\mathrm{s}}^{-\frac{n}{2}-1}\right)\cos\left(\frac{n}{2}\theta\right)\right] \end{aligned} \tag{39}$$

On the stator side, the tangential component of magnetic field intensity can be described as

$$H_{\theta \mathrm{III}}(R_{\mathrm{s}}) = \begin{cases} H_{\theta \mathrm{III}i}(R_{\mathrm{s}}), \theta_i \le \theta \le \theta_i + \beta (\text{stator slots}) \\ 0, \quad \text{elsewhere} \quad (\text{stator teeth}) \end{cases} \tag{40}$$

where the tangential component of magnetic field intensity at the ith slot opening is

$$\begin{aligned} H_{\theta \mathrm{III}i}(R_{\mathrm{s}}) &= -\frac{1}{\mu_0}\frac{\partial A_{\mathrm{III}i}}{\partial r}\bigg|_{r=R_{\mathrm{s}}} \\ &= -\frac{1}{\mu_0}\sum_{k=1}^{\infty} G_{\mathrm{III}ik} Y_k \frac{1}{R_{\mathrm{s}}}\left[\left(\frac{R_{\mathrm{s}}}{R_{\mathrm{sb}}}\right)^{Y_k} - \left(\frac{R_{\mathrm{s}}}{R_{\mathrm{sb}}}\right)^{-Y_k}\right]\cos[Y_k(\theta - \theta_i)] \\ i = 1, 2, \ldots, Q \ \&\ \theta_i \le \theta \le \theta_i + \beta \end{aligned} \tag{41}$$

To solve (38), $H_{\theta \mathrm{III}}(R_{\mathrm{s}})$ is expanded into Fourier's series over the entire circumference:

$$H_{\theta \mathrm{III}}(R_{\mathrm{s}}) = \sum_{n=1}^{\infty} h_{sn} \sin\left(\frac{n}{2}\theta\right) + \sum_{n=1}^{\infty} h_{cn} \cos\left(\frac{n}{2}\theta\right) \tag{42}$$

where the Fourier coefficients can be expressed as

$$h_{sn}=\frac{1}{2\pi}\sum_{i=1}^{Q}\int_{\theta_i}^{\theta_i+\beta}H_{\theta\mathrm{III}i}(R_\mathrm{s})\sin\left(\frac{n}{2}\theta\right)\mathrm{d}\theta$$
$$=\sum_{i=1}^{Q}\sum_{k=1}^{\infty}\frac{1}{2\pi}\left(-\frac{1}{\mu_0}\right)G_{\mathrm{III}ik}Y_k\frac{1}{R_\mathrm{s}}\left[\left(\frac{R_\mathrm{s}}{R_\mathrm{sb}}\right)^{Y_k}-\left(\frac{R_\mathrm{s}}{R_\mathrm{sb}}\right)^{-Y_k}\right] \quad (43a)$$
$$\int_{\theta_i}^{\theta_i+\beta}\cos[Y_k(\theta-\theta_i)]\sin\left(\frac{n}{2}\theta\right)\mathrm{d}\theta$$

$$h_{cn}=\frac{1}{2\pi}\sum_{i=1}^{Q}\int_{\theta_i}^{\theta_i+\beta}H_{\theta\mathrm{III}i}(R_\mathrm{s})\cos\left(\frac{n}{2}\theta\right)\mathrm{d}\theta$$
$$=\sum_{i=1}^{Q}\sum_{k=1}^{\infty}\frac{1}{2\pi}\left(-\frac{1}{\mu_0}\right)G_{\mathrm{III}ik}Y_k\frac{1}{R_\mathrm{s}}\left[\left(\frac{R_\mathrm{s}}{R_\mathrm{sb}}\right)^{Y_k}-\left(\frac{R_\mathrm{s}}{R_\mathrm{sb}}\right)^{-Y_k}\right] \quad (43b)$$
$$\int_{\theta_i}^{\theta_i+\beta}\cos[Y_k(\theta-\theta_i)]\cos\left(\frac{n}{2}\theta\right)\mathrm{d}\theta$$

By comparing the expressions of $H_{\theta\mathrm{II}}(R_\mathrm{s})$ (39) and $H_{\theta\mathrm{III}}(R_\mathrm{s})$ (42), the following relations are obtained:

$$\sum_{i=1}^{Q}\sum_{k=1}^{\infty}\frac{1}{2\pi}G_{\mathrm{III}ik}Y_k\frac{1}{R_\mathrm{s}}\left[\left(\frac{R_\mathrm{s}}{R_\mathrm{sb}}\right)^{Y_k}-\left(\frac{R_\mathrm{s}}{R_\mathrm{sb}}\right)^{-Y_k}\right]$$
$$\int_{\theta}^{\theta_i+\beta}\cos[Y_k(\theta-\theta_i)]\sin\left(\frac{n}{2}\theta\right)\mathrm{d}\theta=\frac{n}{2}\left(E_{\mathrm{II}n}R_\mathrm{s}^{\frac{n}{2}-1}-F_{\mathrm{II}n}R_\mathrm{s}^{-\frac{n}{2}-1}\right) \quad (44a)$$

$$\sum_{i=1}^{Q}\sum_{k=1}^{\infty}\frac{1}{2\pi}G_{\mathrm{III}ik}Y_k\frac{1}{R_\mathrm{s}}\left[\left(\frac{R_\mathrm{s}}{R_\mathrm{sb}}\right)^{Y_k}-\left(\frac{R_\mathrm{s}}{R_\mathrm{sb}}\right)\right]^{-Y_k}$$
$$\int_{\theta_i}^{\theta_i+\beta}\cos[Y_k(\theta-\theta_i)]\cos\left(\frac{n}{2}\theta\right)\mathrm{d}\theta=\frac{n}{2}\left(C_{\mathrm{II}n}R_\mathrm{s}^{\frac{n}{2}-1}-D_{\mathrm{II}n}R_\mathrm{s}^{-\frac{n}{2}-1}\right) \quad (44b)$$

The above process shows the reason why at the beginning we expanded M_r and M_θ into Fourier's series over the entire circumference, so that two equations (39) and (42) have the same variables format and can be compared.

Also, it can be seen from (44) that the left sides are the sum about all slots, which means the magnetic field distributions of all slots are coupled together. This is the essence of the exact magnetic field computation.

b) At the slots opening of this interface, the radial components of flux density are continuous, i.e.,

$$B_{\mathrm{rII}}=B_{\mathrm{rIII}i},\ r=R_\mathrm{s},\ i=1,2,\ldots,Q\ \&\ \theta_i\le\theta\le\theta_i+\beta \quad (45)$$

On the slots side, the radial component of flux density is

$$B_{\mathrm{rIII}i}(R_\mathrm{s})=\frac{1}{r}\frac{\partial A_{\mathrm{III}i}}{\partial\theta}\bigg|_{R_\mathrm{s}}$$
$$=\frac{1}{R_\mathrm{s}}\sum_{k=1}^{\infty}-G_{\mathrm{III}ik}\left[\left(\frac{R_\mathrm{s}}{R_\mathrm{sb}}\right)^{Y_k}+\left(\frac{R_\mathrm{s}}{R_\mathrm{sb}}\right)^{-Y_k}\right]Y_k\sin[Y_k(\theta-\theta_i)],$$
$$i=1,2,\ldots,Q\ \&\ \theta_i\le\theta\le\theta_i+\beta \quad (46)$$

On the air gap side, the radial component of flux density is

$$B_{\mathrm{rII}}(R_\mathrm{s})=\frac{1}{r}\frac{\partial A_{\mathrm{II}}}{\partial\theta}\bigg|_{r=R_\mathrm{s}}=\frac{1}{R_\mathrm{s}}\left\{\sum_{n=1}^{\infty}\frac{n}{2}\left(E_{\mathrm{II}n}R_\mathrm{s}^{\frac{n}{2}}+F_{\mathrm{II}n}R_\mathrm{s}^{-\frac{n}{2}}\right)\cos\left(\frac{n}{2}\theta\right)\right.$$
$$\left.+\sum_{n=1}^{\infty}-\frac{n}{2}\left(C_{\mathrm{II}n}R_\mathrm{s}^{\frac{n}{2}}+D_{\mathrm{II}n}R_\mathrm{s}^{-\frac{n}{2}}\right)\sin\left(\frac{n}{2}\theta\right)\right\} \quad (47)$$

To solve (45), $B_{\mathrm{rII}}(R_\mathrm{s})$ is expanded into Fourier's series over the ith slot opening:

$$B_{\mathrm{rII}i}(R_\mathrm{s})=\sum_{k=1}^{\infty}b_{ik}\sin[Y_k(\theta-\theta_i)],$$
$$i=1,2,\ldots,Q\ \&\ \theta_i\le\theta\le\theta_i+\beta \quad (48)$$

where the Fourier coefficients can be expressed as

$$b_{ik}=\frac{2}{\beta}\int_{\theta_i}^{\theta_i+\beta}B_{r1}(R_\mathrm{s})\sin[Y_k(\theta-\theta_i)]\mathrm{d}\theta$$
$$=\sum_{n=1}^{\infty}\frac{2}{\beta}\frac{1}{r}\frac{n}{2}(E_{\mathrm{II}n}R_\mathrm{s}^{\frac{n}{2}}+F_{\mathrm{II}n}R_\mathrm{s}^{-\frac{n}{2}})\int_{\theta_i}^{\theta_i+\beta}\cos(\frac{n}{2}\theta)\sin[Y_k(\theta-\theta_i)]\mathrm{d}\theta$$
$$+\sum_{n=1}^{\infty}-\frac{2}{\beta}\frac{1}{r}\frac{n}{2}(C_{\mathrm{II}n}R_\mathrm{s}^{\frac{n}{2}}+D_{\mathrm{II}n}R_\mathrm{s}^{-\frac{n}{2}})\int_{\theta_i}^{\theta_i+\beta}\sin(\frac{n}{2}\theta)\sin[Y_k(\theta-\theta_i)]\mathrm{d}\theta \quad (49)$$

By comparing the expressions of $B_{\mathrm{rIII}i}(R_\mathrm{s})$ (46) and $B_{\mathrm{rII}i}(R_\mathrm{s})$ (48), the following relation is obtained:

$$\sum_{n=1}^{\infty}\frac{2}{\beta}\frac{n}{2}\left(E_{\mathrm{II}n}R_\mathrm{s}^{\frac{n}{2}}+F_{\mathrm{II}n}R_\mathrm{s}^{-\frac{n}{2}}\right)\int_{\theta_i}^{\theta_i+\beta}\cos\left(\frac{n}{2}\theta\right)\sin[Y_k(\theta-\theta_i)]\mathrm{d}\theta$$
$$+\sum_{n=1}^{\infty}-\frac{2}{\beta}\frac{n}{2}\left(C_{\mathrm{II}n}R_\mathrm{s}^{\frac{n}{2}}+D_{\mathrm{II}n}R_\mathrm{s}^{-\frac{n}{2}}\right)\int_{\theta_i}^{\theta_i+\beta}\sin\left(\frac{n}{2}\theta\right)\sin[Y_k(\theta-\theta_i)]\mathrm{d}\theta,$$
$$=-G_{\mathrm{III}ik}Y_k\left[\left(\frac{R_\mathrm{s}}{R_\mathrm{sb}}\right)^{Y_k}+\left(\frac{R_\mathrm{s}}{R_\mathrm{sb}}\right)^{-Y_k}\right]$$
$$i=1,2,\ldots,Q\ \&\ \theta_i\le\theta\le\theta_i+\beta \quad (50)$$

Note that this equation should be applied to every slot if the stator has Q slots.

2.5. Solving equations

At the three interfaces $r=R_\mathrm{r}$, $r=R_\mathrm{m}$, and $r=R_\mathrm{s}$, there are five boundary conditions for the magnetic field, and five equations (31), (34), (37), (44), and (50) are obtained accordingly. Theoretically, solving those equations can determine all unknowns $C_{\mathrm{I}n}$, $D_{\mathrm{I}n}$, $E_{\mathrm{I}n}$, $F_{\mathrm{I}n}$, $C_{\mathrm{II}n}$, $D_{\mathrm{II}n}$, $E_{\mathrm{II}n}$, $F_{\mathrm{II}n}$ and $G_{\mathrm{III}ik}$, but it can be seen it is not very easy due to the complex expressions of the equations. Here, one solving process we used is introduced.

At the boundary conditions 1) $r=R_\mathrm{r}$ and 2) $r=R_\mathrm{m}$, equations (31a), (34a), and (37a) are only related with the unknowns $E_{\mathrm{II}n}$, $F_{\mathrm{II}n}$, $E_{\mathrm{I}n}$, and $F_{\mathrm{I}n}$, and equations (31b), (34b), and (37b) are only related with the unknowns $C_{\mathrm{I}n}$, $D_{\mathrm{I}n}$, $C_{\mathrm{II}n}$, and $D_{\mathrm{II}n}$. Hence, the relations between $E_{\mathrm{II}n}$, $F_{\mathrm{II}n}$, $E_{\mathrm{I}n}$, and $F_{\mathrm{I}n}$, and the relations between $C_{\mathrm{I}n}$, $D_{\mathrm{I}n}$, $C_{\mathrm{II}n}$, and

$D_{\mathrm{II}n}$, can be respectively deduced by those two sets of equations:

$$F_{1n}=\begin{cases}\left\{\begin{matrix}E_{\mathrm{II}n}R_{\mathrm{m}}^{\frac{n}{2}}+F_{\mathrm{II}n}R_{\mathrm{m}}^{-\frac{n}{2}}+\dfrac{\mu_0}{n^2-4}\\ [R_{\mathrm{m}}^{\frac{n}{2}}R_{\mathrm{r}}^{1-\frac{n}{2}}(4M_{rnc}+2nM_{\theta ns})-2R_{\mathrm{m}}(nM_{rnc}+2M_{\theta ns})]\end{matrix}\right\}\dfrac{R_{\mathrm{m}}^{\frac{n}{2}}R_{\mathrm{r}}^{n}}{R_{\mathrm{m}}^{n}+R_{\mathrm{r}}^{n}},\\ n=1,3,4,...\\ \left\{\begin{matrix}E_{\mathrm{II}n}R_{\mathrm{m}}+F_{\mathrm{II}n}R_{\mathrm{m}}^{-1}+\dfrac{\mu_0 R_{\mathrm{m}}}{2}\\ [M_{\theta ns}(1+\ln\dfrac{R_{\mathrm{m}}}{R_{\mathrm{r}}})+M_{rnc}(-1+\ln\dfrac{R_{\mathrm{m}}}{R_{\mathrm{r}}})]\end{matrix}\right\}\dfrac{R_{\mathrm{m}}R_{\mathrm{r}}^{2}}{R_{\mathrm{m}}^{2}+R_{\mathrm{r}}^{2}},n=2\end{cases}\tag{51a}$$

$$E_{1n}=\begin{cases}\dfrac{1}{R_{\mathrm{r}}^{n}}F_{1n}-\dfrac{R_{\mathrm{r}}^{1-\frac{n}{2}}\mu_0(4M_{rnc}+2nM_{\theta ns})}{n^2-4},n=1,3,4,...\\ \dfrac{1}{R_{\mathrm{r}}^{2}}F_{1n}+\dfrac{\mu_0}{2}\left[M_{\theta ns}(-1+\ln R_{\mathrm{r}})+M_{rnc}(1+\ln R_{\mathrm{r}})\right],n=2\end{cases}\tag{51b}$$

$$D_{1n}=\begin{cases}\left\{\begin{matrix}C_{\mathrm{II}n}R_{\mathrm{m}}^{\frac{n}{2}}+D_{\mathrm{II}n}R_{\mathrm{m}}^{-\frac{n}{2}}-\dfrac{\mu_0}{n^2-4}\\ [R_{\mathrm{m}}^{\frac{n}{2}}R_{\mathrm{r}}^{1-\frac{n}{2}}(4M_{rns}-2nM_{\theta nc})-2R_{\mathrm{m}}(nM_{rns}-2M_{\theta nc})]\end{matrix}\right\}\dfrac{R_{\mathrm{m}}^{\frac{n}{2}}R_{\mathrm{r}}^{n}}{R_{\mathrm{m}}^{n}+R_{\mathrm{r}}^{n}},\\ n=1,3,4,..\\ \left\{\begin{matrix}C_{\mathrm{II}n}R_{\mathrm{m}}+D_{\mathrm{II}n}R_{\mathrm{m}}^{-1}+\dfrac{\mu_0 R_{\mathrm{m}}}{2}\\ [M_{\theta nc}(1+\ln\dfrac{R_{\mathrm{m}}}{R_{\mathrm{r}}})-M_{rns}(-1+\ln\dfrac{R_{\mathrm{m}}}{R_{\mathrm{r}}})]\end{matrix}\right\}\dfrac{R_{\mathrm{m}}R_{\mathrm{r}}^{2}}{R_{\mathrm{m}}^{2}+R_{\mathrm{r}}^{2}},n=2\end{cases}\tag{51c}$$

$$C_{1n}=\begin{cases}\dfrac{1}{R_{\mathrm{r}}^{n}}D_{1n}+\dfrac{R_{\mathrm{r}}^{1-\frac{n}{2}}\mu_0(4M_{rns}-2nM_{\theta nc})}{n^2-4},n=1,3,4,...\\ \dfrac{1}{R_{\mathrm{r}}^{2}}D_{1n}+\dfrac{\mu_0}{2}\left[M_{\theta nc}(-1+\ln R_{\mathrm{r}})-M_{rns}(1+\ln R_{\mathrm{r}})\right],n=2\end{cases}\tag{51d}$$

The relation between $E_{\mathrm{II}n}$ and $F_{\mathrm{II}n}$, and the relation between $C_{\mathrm{II}n}$ and $D_{\mathrm{II}n}$, are as follows:

$$F_{\mathrm{II}n}=\varepsilon_E E_{\mathrm{II}n}+\sigma_E\tag{52a}$$

$$D_{\mathrm{II}n}=\varepsilon_C C_{\mathrm{II}n}+\sigma_C\tag{52b}$$

where

$$\varepsilon_E=\varepsilon_C=\frac{R_{\mathrm{m}}^{n}(R_{\mathrm{r}}^{n}-R_{\mathrm{m}}^{n}+\mu_{\mathrm{r}}R_{\mathrm{m}}^{n}+\mu_{\mathrm{r}}R_{\mathrm{r}}^{n})}{R_{\mathrm{m}}^{n}-R_{\mathrm{r}}^{n}+\mu_{\mathrm{r}}R_{\mathrm{m}}^{n}+\mu_{\mathrm{r}}R_{\mathrm{r}}^{n}}\tag{53a}$$

$$\sigma_E=\begin{cases}\dfrac{R_{\mathrm{m}}R_{\mathrm{r}}^{n}(2+n)(M_{rnc}+M_{\theta ns})+R_{\mathrm{m}}^{n+1}(2-n)(M_{rnc}-M_{\theta ns})}{-2R_{\mathrm{m}}^{\frac{n}{2}}\mu_0\dfrac{-R_{\mathrm{m}}^{\frac{n}{2}}R_{\mathrm{r}}^{\frac{n}{2}+1}(4M_{rnc}+2nM_{\theta ns})}{(n^2-4)(R_{\mathrm{m}}^{n}-R_{\mathrm{r}}^{n}+\mu_{\mathrm{r}}R_{\mathrm{m}}^{n}+\mu_{\mathrm{r}}R_{\mathrm{r}}^{n})}},\\ n=1,3,4,...\\ -R_{\mathrm{m}}^{2}\mu_0\dfrac{(R_{\mathrm{m}}^{2}-R_{\mathrm{r}}^{2})(M_{\theta ns}-M_{rnc})+2R_{\mathrm{r}}^{2}(M_{rnc}+M_{\theta ns})\ln(\dfrac{R_{\mathrm{r}}}{R_{\mathrm{m}}})}{2(R_{\mathrm{m}}^{2}-R_{\mathrm{r}}^{2}+\mu_{\mathrm{r}}R_{\mathrm{m}}^{2}+\mu_{\mathrm{r}}R_{\mathrm{r}}^{2})},n=2\end{cases}\tag{53b}$$

$$\sigma_C=\begin{cases}\dfrac{R_{\mathrm{m}}R_{\mathrm{r}}^{n}(2+n)(M_{rns}-M_{\theta nc})+R_{\mathrm{m}}^{n+1}(2-n)(M_{\theta nc}+M_{rns})}{2R_{\mathrm{m}}^{\frac{n}{2}}\mu_0\dfrac{-R_{\mathrm{m}}^{\frac{n}{2}}R_{\mathrm{r}}^{\frac{n}{2}+1}(4M_{rns}-2nM_{\theta nc})}{(n^2-4)(R_{\mathrm{m}}^{n}-R_{\mathrm{r}}^{n}+\mu_{\mathrm{r}}R_{\mathrm{m}}^{n}+\mu_{\mathrm{r}}R_{\mathrm{r}}^{n})}},\\ n=1,3,4,...\\ -R_{\mathrm{m}}^{2}\mu_0\dfrac{(R_{\mathrm{m}}^{2}-R_{\mathrm{r}}^{2})(M_{\theta nc}+M_{rns})+2R_{\mathrm{r}}^{2}(M_{\theta nc}-M_{rns})\ln(\dfrac{R_{\mathrm{r}}}{R_{\mathrm{m}}})}{2(R_{\mathrm{m}}^{2}-R_{\mathrm{r}}^{2}+\mu_{\mathrm{r}}R_{\mathrm{m}}^{2}+\mu_{\mathrm{r}}R_{\mathrm{r}}^{2})},n=2\end{cases}\tag{53c}$$

By substituting the expression of $F_{\mathrm{II}n}$ (52a) into the condition (44a), and then it only includes the unknowns $G_{\mathrm{III}ik}$ and $E_{\mathrm{II}n}$, and can be rewritten as

$$w_E(n)E_{\mathrm{II}n}-\sum_{i=1}^{Q}\sum_{k=1}^{\infty}u_E(n,i,k)G_{\mathrm{III}ik}=-\delta_E(n)\tag{54}$$

where

$$w_E(n)=\frac{n}{2}\left(R_{\mathrm{s}}^{\frac{n}{2}-1}-\varepsilon_E R_{\mathrm{s}}^{-\frac{n}{2}-1}\right)\tag{55a}$$

$$\delta_E(n)=-\frac{n}{2}\sigma_E R_{\mathrm{s}}^{-\frac{n}{2}-1}\tag{55b}$$

$$u_E(n,i,k)=\frac{1}{2\pi}Y_k\frac{1}{R_{\mathrm{s}}}\left[\left(\frac{R_{\mathrm{s}}}{R_{\mathrm{sb}}}\right)^{Y_k}-\left(\frac{R_{\mathrm{s}}}{R_{\mathrm{sb}}}\right)^{-Y_k}\right]\int_{\theta_i}^{\theta_i+\beta}\cos[Y_k(\theta-\theta_i)\sin\left(\frac{n}{2}\theta\right)\mathrm{d}\theta\tag{55c}$$

In actual computation, finite terms of Fourier's series are utilized, i.e., n = 1, 2, 3…, N; k = 1, 2, 3,…, K; where N and K are the highest harmonic order. Equation (54) can be written into a matrix format

$$\mathbf{w_E}\mathbf{E_{II}}-\mathbf{u_E}\mathbf{G_{III}}=-\boldsymbol{\delta}_{\mathbf{E}}\tag{56}$$

where

$$\mathbf{w_E}=\mathrm{diag}[w_E(1),w_E(2),\cdots,w_E(n),\cdots,w_E(N)]_{N\times N}\tag{57a}$$

$$\mathbf{E_{II}}=[E_{\mathrm{II}1},E_{\mathrm{II}2},\cdots,E_{\mathrm{II}n},\cdots,E_{\mathrm{II}N}]^{\mathrm{T}}\tag{57b}$$

$$\begin{cases}\mathbf{u_E}=[\mathbf{u_{E1}},\mathbf{u_{E2}},\cdots,\mathbf{u_{En}},\cdots,\mathbf{u_{EN}}]^{\mathrm{T}}\\ \mathbf{u_{En}}=[\mathbf{u_{En1}},\mathbf{u_{En2}},\cdots,\mathbf{u_{Eni}},\cdots,\mathbf{u_{EnQ}}]^{\mathrm{T}}\\ \mathbf{u_{Eni}}=[u_E(n,i,1),u_E(n,i,2),\cdots,u_E(n,i,k),\cdots,u_E(n,i,K)]\end{cases}\tag{57c}$$

$$\begin{cases}\mathbf{G_{III}}=[\mathbf{G_{III1}},\mathbf{G_{III2}},\cdots,\mathbf{G_{IIIi}},\cdots,\mathbf{G_{IIIQ}}]^{\mathrm{T}}\\ \mathbf{G_{IIIi}}=[G_{\mathrm{III}i1},G_{\mathrm{III}i2},\cdots,G_{\mathrm{III}ik},\cdots,G_{\mathrm{III}iK}]\end{cases}\tag{57d}$$

$$\boldsymbol{\delta}_{\mathbf{E}}=[\delta_E(1),\delta_E(2),\cdots,\delta_E(n),\cdots,\delta_E(N)]^{\mathrm{T}}\tag{57e}$$

Likewise, substituting the expression of $D_{\mathrm{II}n}$ (52b) into the condition (44b), and then it only includes the unknowns $G_{\mathrm{III}ik}$ and $C_{\mathrm{II}n}$, and can be rewritten as

$$w_C(n)C_{\mathrm{II}n} - \sum_{i=1}^{Q}\sum_{k=1}^{\infty} u_C(n,i,k)G_{\mathrm{III}ik} = -\delta_C(n) \tag{58}$$

where

$$w_C(n) = \frac{n}{2}\left(R_{\mathrm{s}}^{\frac{n}{2}-1} - \varepsilon_C R_{\mathrm{s}}^{-\frac{n}{2}-1}\right) \tag{59a}$$

$$\delta_C(n) = -\frac{n}{2}\sigma_C R_{\mathrm{s}}^{-\frac{n}{2}-1} \tag{59b}$$

$$u_C(n,i,k) = \frac{1}{2\pi}Y_k\frac{1}{R_{\mathrm{s}}}\left[\left(\frac{R_{\mathrm{s}}}{R_{\mathrm{sb}}}\right)^{Y_k} - \left(\frac{R_{\mathrm{s}}}{R_{\mathrm{sb}}}\right)^{-Y_k}\right] \int_{\theta_i}^{\theta_i+\beta}\cos[Y_k(\theta-\theta_i)]\cos\left(\frac{n}{2}\theta\right)\mathrm{d}\theta \tag{59c}$$

Equation (58) can be written into a matrix format

$$\mathbf{w_C C_{II}} - \mathbf{u_C G_{III}} = -\boldsymbol{\delta}_{\mathbf{C}} \tag{60}$$

where

$$\mathbf{w_C} = \mathrm{diag}[w_C(1), w_C(2), \cdots, w_C(n), \cdots, w_C(N)]_{N\times N} \tag{61a}$$

$$\mathbf{C_{II}} = [C_{\mathrm{II}1}, C_{\mathrm{II}2}, \cdots, C_{\mathrm{II}n}, \cdots, C_{\mathrm{II}N}]^{\mathrm{T}} \tag{61b}$$

$$\begin{cases} \mathbf{u_C} = [\mathbf{u_{C1}}, \mathbf{u_{C2}}, \cdots, \mathbf{u_{Cn}}, \cdots, \mathbf{u_{CN}}]^{\mathrm{T}} \\ \mathbf{u_{Cn}} = [\mathbf{u_{Cn1}}, \mathbf{u_{Cn2}}, \cdots, \mathbf{u_{Cni}}, \cdots, \mathbf{u_{CnQ}}]^{\mathrm{T}} \\ \mathbf{u_{Cni}} = [u_C(n,i,1), u_C(n,i,2), \cdots, u_C(n,i,k), \cdots, u_C(n,i,K)] \end{cases} \tag{61c}$$

$$\boldsymbol{\delta}_{\mathbf{C}} = [\delta_C(1), \delta_C(2), \cdots, \delta_C(n), \cdots, \delta_C(N)]^{\mathrm{T}} \tag{61d}$$

Similarly, substituting the expressions of both $E_{\mathrm{II}n}$ (52a) and $D_{\mathrm{II}n}$ (52b) into the condition (50), and then it is only related with the unknowns $G_{\mathrm{III}ik}$, $E_{\mathrm{II}n}$, and $C_{\mathrm{II}n}$, and can be rewritten as

$$\sum_{n=1}^{\infty}[v_E(n,i,k)E_{\mathrm{II}n} + v_C(n,i,k)C_{\mathrm{II}n}] - u_{EC}(k)G_{\mathrm{III}ik} = -\sum_{n=1}^{\infty}\delta_{EC}(n,i,k) \tag{62}$$

where

$$\delta_{EC}(n,i,k) = \sigma_E R_{\mathrm{s}}^{-\frac{n}{2}}\zeta_E(n,i,k) + \sigma_C R_{\mathrm{s}}^{-\frac{n}{2}}\zeta_C(n,i,k) \tag{63a}$$

$$u_{EC}(k) = -Y_k\left[\left(\frac{R_{\mathrm{s}}}{R_{\mathrm{sb}}}\right)^{Y_k} + \left(\frac{R_{\mathrm{s}}}{R_{\mathrm{sb}}}\right)^{-Y_k}\right] \tag{63b}$$

$$v_E(n,i,k) = \left(R_{\mathrm{s}}^{\frac{n}{2}} + \varepsilon_E R_{\mathrm{s}}^{-\frac{n}{2}}\right)\zeta_E(n,i,k) \tag{63c}$$

$$v_C(n,i,k) = \left(R_{\mathrm{s}}^{\frac{n}{2}} + \varepsilon_C R_{\mathrm{s}}^{-\frac{n}{2}}\right)\zeta_C(n,i,k) \tag{63d}$$

with

$$\zeta_E(n,i,k) = \frac{2}{\beta}\frac{n}{2}\int_{\theta_i}^{\theta_i+\beta}\cos\left(\frac{n}{2}\theta\right)\sin[Y_k(\theta-\theta_i)]\mathrm{d}\theta \tag{64a}$$

$$\zeta_C(n,i,k) = -\frac{2}{\beta}\frac{n}{2}\int_{\theta_i}^{\theta_i+\beta}\sin\left(\frac{n}{2}\theta\right)\sin[Y_k(\theta-\theta_i)]\mathrm{d}\theta \tag{64b}$$

Rewrite (62) into matrix format

$$\mathbf{v_E E_{II}} + \mathbf{v_C C_{II}} - \mathbf{u_{EC} G_{III}} = -\boldsymbol{\delta}_{\mathbf{EC}} \tag{65}$$

where

$$\begin{cases} \mathbf{v_E} = [\mathbf{v_{E1}}, \mathbf{v_{E2}}, \cdots, \mathbf{v_{Ei}}, \cdots, \mathbf{v_{EQ}}]^{\mathrm{T}} \\ \mathbf{v_{Ei}} = [\mathbf{v_{Ei1}}, \mathbf{v_{Ei2}}, \cdots, \mathbf{v_{Eik}}, \cdots, \mathbf{v_{EiK}}] \\ \mathbf{v_{Eik}} = [v_E(1,i,k), v_E(2,i,k), \cdots, v_E(n,i,k), \cdots, v_E(N,i,k)]^{\mathrm{T}} \end{cases} \tag{66a}$$

$$\begin{cases} \mathbf{v_C} = [\mathbf{v_{C1}}, \mathbf{v_{C2}}, \cdots, \mathbf{v_{Ci}}, \cdots, \mathbf{v_{CQ}}]^{\mathrm{T}} \\ \mathbf{v_{Ci}} = [\mathbf{v_{Ci1}}, \mathbf{v_{Ci2}}, \cdots, \mathbf{v_{Cik}}, \cdots, \mathbf{v_{CiK}}] \\ \mathbf{v_{Cik}} = [v_C(1,i,k), v_C(2,i,k), \cdots, v_C(n,i,k), \cdots, v_C(N,i,k)]^{\mathrm{T}} \end{cases} \tag{66b}$$

$$\begin{cases} \mathbf{u_{EC}} = \mathrm{diag}[\mathbf{u_{EC1}}, \mathbf{u_{EC2}}, \cdots, \mathbf{u_{ECi}}, \cdots, \mathbf{u_{ECQ}}]_{Q\times Q} \\ \mathbf{u_{ECi}} = \mathrm{diag}[u_{EC}(1), u_{EC}(2), \cdots, u_{EC}(k), \cdots, u_{EC}(K)]_{K\times K} \end{cases} \tag{66c}$$

$$\begin{cases} \boldsymbol{\delta}_{\mathbf{EC}} = [\boldsymbol{\delta}_{\mathbf{EC1}}, \boldsymbol{\delta}_{\mathbf{EC2}}, \cdots, \boldsymbol{\delta}_{\mathbf{ECi}}, \cdots, \boldsymbol{\delta}_{\mathbf{ECQ}}]^{\mathrm{T}} \\ \boldsymbol{\delta}_{\mathbf{ECi}} = [\delta_{ECi1}, \delta_{ECi2}, \cdots, \delta_{ECik}, \cdots, \delta_{ECiK}] \\ \delta_{ECik} = [\delta_{EC}(1,i,k), \delta_{EC}(2,i,k), \cdots, \delta_{EC}(n,i,k), \cdots, \delta_{EC}(N,i,k)]_{1\times N}[1,1,\cdots,1]^{\mathrm{T}}_{N\times 1} \end{cases} \tag{66d}$$

Combining (56), (60) and (65), the final matrix equation is obtained:

$$\begin{pmatrix} \mathbf{w_E} & \mathbf{0} & -\mathbf{u_E} \\ \mathbf{0} & \mathbf{w_C} & -\mathbf{u_C} \\ \mathbf{v_E} & \mathbf{v_C} & -\mathbf{u_{EC}} \end{pmatrix}\begin{pmatrix} \mathbf{E_{II}} \\ \mathbf{C_{II}} \\ \mathbf{G_{III}} \end{pmatrix} = \begin{pmatrix} -\boldsymbol{\delta}_{\mathbf{E}} \\ -\boldsymbol{\delta}_{\mathbf{C}} \\ -\boldsymbol{\delta}_{\mathbf{EC}} \end{pmatrix} \tag{67}$$

It is a non-homogeneous linear system and contains $2N+QK$ equations with $2N+QK$ unknowns. By this set of simultaneous equations, the unknown coefficients $E_{\mathrm{II}n}$, $C_{\mathrm{II}n}$, and $G_{\mathrm{III}ik}$ can be solved, then $F_{\mathrm{II}n}$ and $D_{\mathrm{II}n}$ can be calculated by (52a) and (52b), and $F_{\mathrm{I}n}$, $E_{\mathrm{I}n}$, $D_{\mathrm{I}n}$, and $C_{\mathrm{I}n}$ can be calculated by (51a), (51b), (51c), and (51d) respectively. Thus, all unknown coefficients are determined. Substituting these obtained coefficients into magnetic field governing equations (19), (22), and (27), the complete answers of A_{I}, A_{II}, and $A_{\mathrm{III}i}$ are obtained. Eventually, the distributions of magnetic fields in PMs, air gap, and stator slots are acquired.

3. Comparison of Analytical Method with FEM

We designed a 315 kW 20000 r/min high-speed PM motor used for a blower. The prototype and the internal structure of the designed PM machine are shown in Fig. 3, where the rotor is levitated by two radial active magnetic bearings and an axial active magnetic bearing. The main parameters of the motor are listed in Table 1

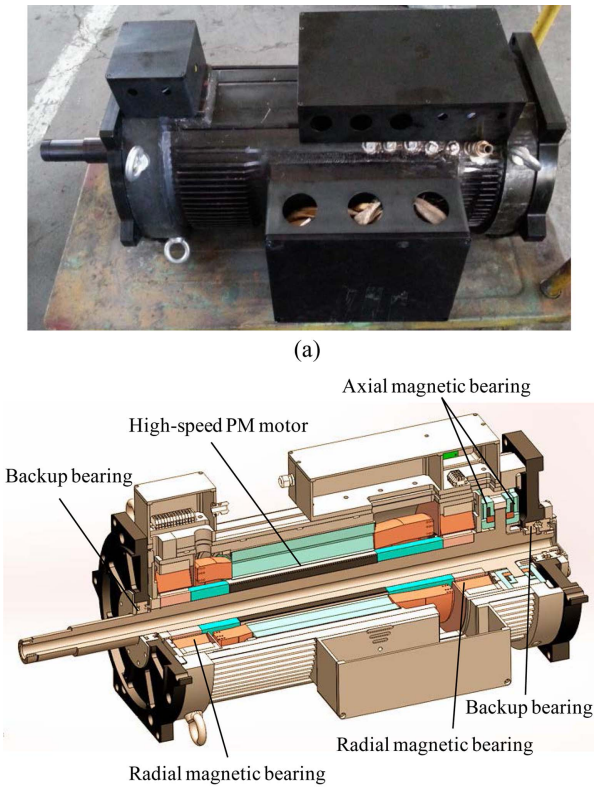

Fig. 3. (Color online) The designed 315 kW 20000 r/min high-speed PM motor (a) Prototype (b) Internal structure.

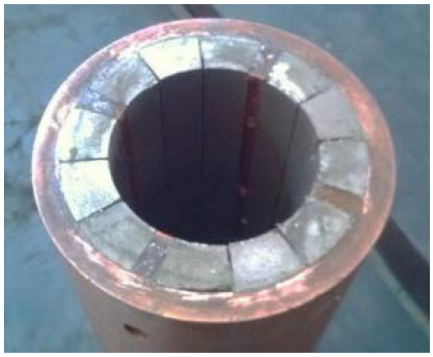

Fig. 4. (Color online) The detail of PMs.

and Table 2. Fig. 4 shows the detail of the magnets in the rotor. It is a four-pole configuration, and each pole is formed by three magnet segments. The material of PMs is Sm_2Co_{17}. In order to facilitate the assembly of magnets, there is a fixed septum with 1 degree between the segmented magnets. The septa between the magnetic poles are designed as 10 degrees.

The magnetic fields in this PM machine are calculated by both analytical method and FEM (in Ansoft Maxwell software). Fig. 5 and Fig. 6 respectively show the flux

Table 1. Main parameters of the designed PM motor.

Symbol	Quantity	Value
R_r	Outer radius of rotor yoke	35 mm
R_m	Outer radius of PMs	51 mm
R_s	Inner radius of stator	61 mm
R_{sb}	Radius of slot bottom	100.7 mm
R	Outer radius of stator	125 mm
L_{fe}	Effective length of motor	290 mm
Q	Number of slots	24
β	Slot opening angle	2.067°
α	Stator tooth angle	12.933°
P	Number of pole pairs	2
J	Number of magnet segments per pole	3
λ_p	Ratio of pole-arc to pole-pitch	0.9
λ_m	Ratio of magnet-arc to magnet-pitch	0.963
B_{rm}	Remanence of PMs	1.05 Tesla
μ_{rm}	Relative recoil permeability of PMs	1.0497

Table 2. Main parameters of the winding.

Winding layers	2	Conductors per slot	6
Parallel branches per phase	4	Coil pitch	6

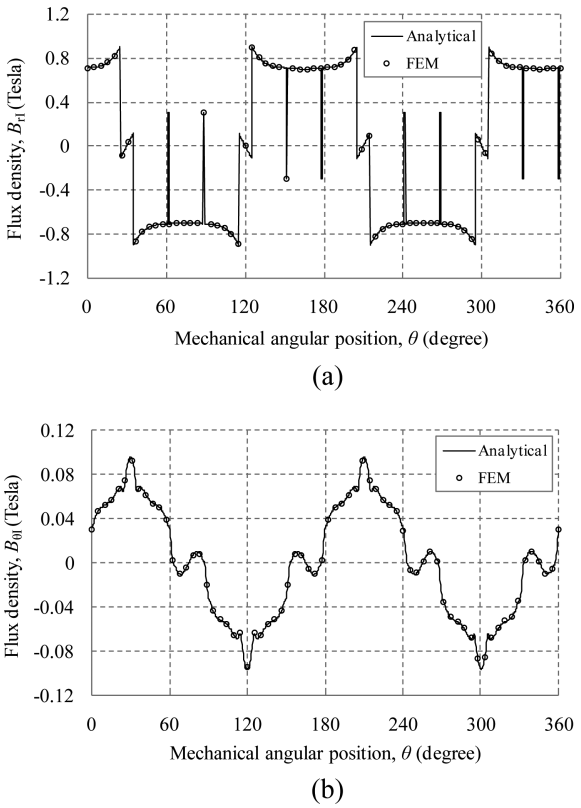

Fig. 5. Flux density distribution in the middle of magnets of the designed PM motor (for rotor angular position is 120° & r = 43 mm) (a) Radial component (b) Tangential component.

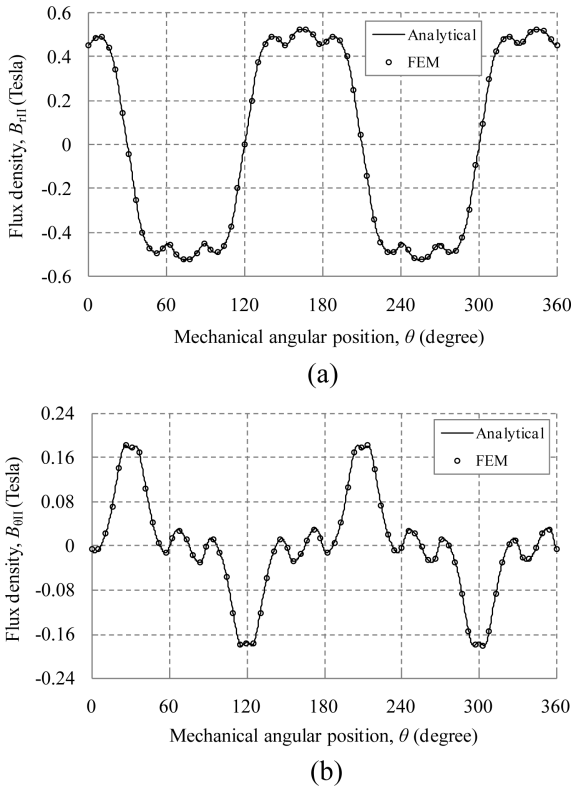

Fig. 6. Flux density distribution in the middle of air gap of the designed PM motor (for rotor angular position is 120° & r = 56 mm) (a) Radial component (b) Tangential component.

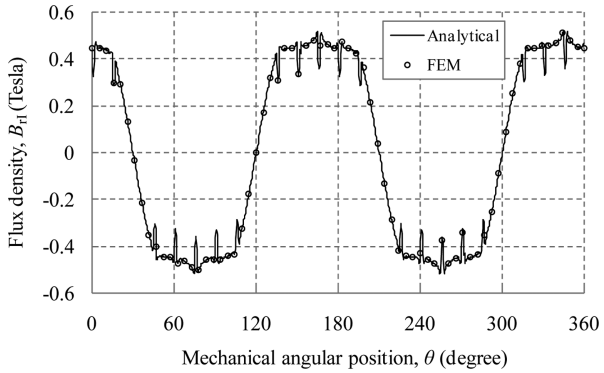

Fig. 7. Flux density distribution in the air gap close to stator bore of the designed PM motor (for rotor angular position is 120° & r = 60.5 mm).

density distributions in the middle of the magnets and air gap when the rotor angular position is 120 degrees, and Fig. 7 shows the flux density distributions in the air gap close to stator bore (at r = 60.5 mm). These results show that the magnetic fields obtained by the analytical model are in good agreement with the FEM, and the slotting effect can be accurately calculated by the presented analytical model.

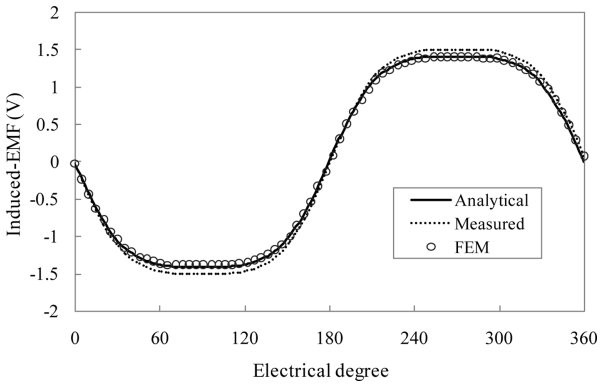

Fig. 8. Phase induced EMF of the designed PM motor with rotor speed 140 r/min.

4. Induced Electromotive Force

As the acquisition of magnetic field distribution, the total magnetic flux through the coils of one phase winding can be calculated by

$$\Phi_{\text{phase}} = \sum_{1}^{N_c} \sum_{\tau=1}^{y} \int_{\theta_\tau}^{\theta_\tau+\alpha} N_t B_{rII}(R_s, \theta) L_{fe} R_s \, d\theta \tag{68}$$

where the starting angular position of the τth tooth is defined as

$$\theta_\tau = \theta_i + \beta \tag{69}$$

L_{fe} is the effective length of the PM machine, α is the stator tooth angle, y is the coil pitch, N_t is the number of turns per coil, and N_c is the number of coils in series per phase. The induced EMF in the windings can be obtained based on Faraday's law

$$E_{\text{phase}} = -\frac{d\Phi_{\text{phase}}}{dt} \tag{70}$$

Fig. 8 shows the phase induced EMF of the designed PM machine when the rotor speed is 140 r/min. There is a good agreement of the results given by analytical method, FEM, and measurement, and the maximum relative error between them is less than 5.1 %, which also indirectly confirms the accuracy of the magnetic field computation. In addition, it can be seen that the waveform of the induced-EMF is close to a flat-top wave for the designed PM machine with three parallelly magnetized magnet segments in each pole, so this PM motor is suited for brushless DC (BLDC) control scheme.

5. Conclusion

In this paper, an analytical solution for calculating the magnetic field in surface-mounted PM machine with

parallelly magnetized magnet segments has been proposed. The magnetic field governing equations, i.e., Poisson's equation in PM region and Laplace's equations in air gap and slots regions, were solved by applying appropriate boundary conditions. The derived analytical solutions were compared with FEM, and the results showed that they were well consistent with each other. In addition, the induced EMF of a designed PM machine was calculated based on the obtained magnetic field solution, and the result was verified by measurement. The presented analytical solution is useful for preliminary design and optimization of the PM machines with parallelly magnetized magnet segments.

References

[1] D. G. Dorrell, M.-F. Hsieh, M. Popescu, L. Evans, D. A. Staton, and V. Grout, IEEE Trans. Ind. Electron. **58**, 3741 (2011).
[2] P.-D. Pfister. and Y. Perriard, IEEE Trans. Ind. Electron. **57**, 296 (2010).
[3] S.-M. Jang, H.-W. Cho, and S.-K. Choi, IEEE Trans. Magn. **43**, 2573 (2007).
[4] X. Zhang and J. Yang, IEEE Trans. Ind. Appl. **54**, 1671 (2018).
[5] C.-C. Hwang, S.-S. Hung, C.-T. Liu, and S.-P. Cheng, IEEE Trans. Magn. **50**, Art. ID 4002304 (2014).
[6] J. Fang and S. Xu, IEEE Trans. Magn. **51**, Art. ID 8207604 (2015).
[7] D. Gerada, A. Mebarki, N. L. Brown, C. Gerada, A. Cavagnino, and A. Boglietti, IEEE Trans. Ind. Electron. **61**, 2946 (2014).
[8] N. Bianchi, S. Bolognani, and F. Luise, IEEE Trans. Ind. Appl. **40**, 1570 (2004).
[9] S. Xu, X. Liu, and Y. Le, IEEE Trans. Magn. **53**, Art. ID 8203715 (2017).
[10] F. Dubas and C. Espanet, IEEE Trans. Magn. **45**, 2097 (2009).
[11] Z. Q. Zhu, L. J. Wu, and Z. P. Xia, IEEE Trans. Magn. **46**, 1100 (2010).
[12] Z. J. Liu and J. T. Li, IEEE Trans. Energy Convers. **23**, 717 (2008).
[13] Z. J. Liu, J. T. Li, and Q. Jiang, J. Appl. Phys. **103**, 07F135 (2008).
[14] T. Lubin, S. Mezani, and A. Rezzoug, IEEE Trans. Magn. **47**, 479 (2011).
[15] L. J. Wu, Z. Q. Zhu, D. Staton, M. Popescu, and D. Hawkins, IEEE Trans. Magn. **47**, 1693 (2011).
[16] T. Lubin, S. Mezani, and A. Rezzoug, IEEE Trans. Magn. **48**, 2080 (2012).
[17] A. Rahideh and T. Korakianitis, IEEE Trans. Magn. **48**, 2633 (2012).
[18] K. Boughrara, R. Ibtiouen, and T. Lubin, IEEE Trans. Magn. **48**, 2121 (2012).
[19] J. Fu and C. Zhu, IEEE Trans. Magn. **48**, 1906 (2012).
[20] Y. Shen and Z. Q. Zhu, IEEE Trans. Magn. **49**, 1461 (2013).
[21] C. Xia, Z. Chen, T. Shi, and H. Wang, IEEE Trans. Magn. **49**, 5112 (2013).
[22] Y. Zhou, H. Li, G. Meng, S. Zhou, and Q. Cao, IEEE Trans. Ind. Electron. **62**, 3438 (2015).
[23] J. D. Ede, K. Atallah, G. W. Jewell, J. B. Wang, and D. Howe, IEEE Trans. Ind. Appl. **43**, 1207 (2007).
[24] M. Mirzaei, A. Binder, B. Funieru, and M. Susic, IEEE Trans. Magn. **48**, 4831 (2012).
[25] P. Sergeant and A. V. d. Bossche, IEEE Trans. Magn. **44**, 4409 (2008).
[26] T. Lubin, S. Mezani, and A. Rezzoug, IEEE Trans. Magn. **46**, 1092 (2010).